Transition to chaos in a confined two-dimensional fluid flow

Transition to Chaos in a Confined Two-Dimensional Fluid Flow

D. Molenaar, H. J. H. Clercx, and G. J. F. van Heijst

Department of Physics, Eindhoven University of Technology, P.O. Box 513, 5600MB Eindhoven, The Netherlands

(Received 17 June 2004; revised manuscript received 13 May 2005; published 2 September 2005)

For a two-dimensional fluid in a square domain with no-slip walls, new direct numerical simulations reveal that the transition from steady to chaotic flow occurs through a sequence of various periodic and quasiperiodic flows, similar to the well-known Ruelle-Takens-Newhouse scenario. For all solutions beyond the ground state, the phenomenology is dominated by a domain-filling circulation cell, whereas the associated symmetry is reduced from the full symmetry group of the square to rotational symmetry over an angle π. The results complement both laboratory experiments in containers with rigid walls and numerical simulations on double-periodic domains.

DOI: 10.1103/PhysRevLett.95.104503 PACS numbers: 47.15.Rq, 05.45.Ac

Experiments on quasi-two-dimensional (2D) flows in shallow fluid layers [1,2] and stratified fluids [3], and numerical studies of confined purely 2D flows, revealed the importance of no-slip boundaries as vorticity sources. These confined flows have a remarkably different phenomenology from flows on a double-periodic domain [4–6], with spontaneous spin-up phenomena, observed in computations of decaying and forced 2D flows [5,6] and in quasi-2D turbulence experiments in confined stratified fluids [3], as a striking example. A key issue for such flows is the possible generation of mean-square vorticity, or enstrophy $Z(t) = \int_\Omega \omega^2 dA$, at the no-slip walls, whereas that quantity decays in time on double-periodic domains [7]. Moreover, in continuously forced 2D turbulence of high Reynolds number the kinetic energy of the flow may grow unbounded on a double-periodic domain, whereas it saturates in a confined domain due to the dissipative action of the no-slip walls. Acknowledging the influence of no-slip boundaries on the phenomenology of confined 2D hydrodynamics motivates a more detailed computational investigation of such flows, also for the preturbulent states of motion. In particular, the transition sequence from steady to chaotic flows and the associated phenomenology is largely unexplored for the setting of a square domain with no-slip boundaries and forms the subject for this Letter.

For laboratory experiments on quasi-2D flows in a square container with no-slip walls [1], the transition sequence was described qualitatively in terms of semistable vortex configurations and was shown to depend strongly on the value of the bottom friction parameter. In containers with large aspect ratios the phenomenology of electromagnetically forced quasi-2D flows in shallow fluid layers was dominated by an array of driven vortices [8]. These latter experiments were mimicked in purely 2D computations, with one periodic and one stress-free direction [9], revealing a period-doubling cascade to chaos. Finally, computations on a square 2D domain with two periodic directions, the traditional setting for computational 2D hydrodynamics, revealed a complex transition sequence including traveling waves and several quasiperiodic motions [10].

Complementing both the computations and the laboratory experiments mentioned above, we show in this Letter that for a 2D flow on a square domain with no-slip walls the transition sequence to chaos, as a function of a single control parameter, corresponds to the Ruelle-Takens-Newhouse scenario [11,12]. This transition sequence, observed before in, e.g., Rayleigh-Bénard convection experiments [13–17], consists of a steady state, periodic flow (period-1 limit cycle), two-frequency quasiperiodic flow (2-torus), three-frequency quasiperiodic flow (3-torus), and chaotic flow, respectively.

Our direct numerical simulations were performed with a pseudospectral code, based on Chebyshev polynomials [18], solving the 2D (Navier-Stokes) vorticity equation on the square $[-1, 1]^2$. The initial conditions correspond to zero vorticity for all simulations. An external force excites the flow, which has unit density, with a fixed vorticity amplitude $A_0 = 0.05$ at the Fourier wave number $k_f = 6$ and an additional weak solid-body rotation ($k_f = 0$). This corresponds to a chessboard pattern of $(k_f)^2$ driven monopolar vortices of alternating sign, which carries the full group of reflection and rotation symmetries of the square. The forcing scheme is comparable to the forcing in experimental setups with shallow layers of electrolyte [1,2], whereas it is of smaller scale than the (4, 1)-mode forcing used in computations on a double-periodic domain [10].

The inverse kinematic viscosity times the constant forcing amplitude A_0 serves as the control parameter, $\nu' = (A_0/\nu)$. Increasing its value in discrete steps, our results can be summarized as follows: two steady branches are observed for $\nu' < 37.5$, a period-1 limit cycle for $37.5 \leq \nu' \leq 55.0$, quasiperiodic motion and a phase of frequency locking on the 2-torus for $57.5 \leq \nu' \leq 75.0$, quasiperiodic motion on the 3-torus for $\nu' = 77.5$, and chaos for $80.0 \leq \nu' \leq 85.0$. Computations with forcing wave number $k_f = 4$ revealed the same transition sequence, although the fundamental frequencies of the various (quasi)periodic motions were shifted to different values, as compared to the case with $k_f = 6$. Results are, however, expected to vary within the full (ν', k_f) parameter space.

As the forcing is defined in terms of Fourier modes, it is subsequently converted to Chebyshev polynomials [6]. The number of computational modes and the time step equal either 161^2 and $\delta t = 3.4 \times 10^{-4}$ or 181^2 and $\delta t = 2.7 \times 10^{-4}$, whereas the simulations run up to $T = 1000$ to generate time series of sufficient length. To make sure the computations are well resolved, it was verified that an increase in the number of computational modes had no effect on the phenomenology or the observed frequencies of motion. Also the boundary layer thickness was checked to be well within computational resolution.

Two steady solutions were found under the given parameter values, as opposed to the four steady branches observed for the double-periodic domain [10]. Similar to experiments in electromagnetically driven shallow fluid layers with strong bottom friction [1], the ground or conductive state, found for $\nu' \leq 25.0$, equals essentially the forcing mode with the associated symmetry. The system bifurcates towards a second steady state in the interval $25.0 < \nu' < 37.5$. Analogous to the onset of steady Rayleigh-Bénard convection, with its convection rolls, the flow field in the second steady state consists of a domain-filling circulation cell, with secondary vortices in the corners. This configuration is no longer reflection symmetric.

A Hopf bifurcation leads to time-dependent behavior in the form of a period-1 limit cycle, observed in the interval $37.5 \leq \nu' \leq 55.0$. Upon entering the periodic state, the flow configuration, which is shown in a contour plot of the normalized vorticity field at parameter value $\nu' = 37.5$, Fig. 1(a), remains unaltered. When the control parameter is further increased, however, the overall symmetry is reduced to invariance with respect to rotations over π. The latter symmetry remains unbroken for the remaining values of the control parameter and is clearly observed in a contour plot of the normalized vorticity field, Fig. 1(b), for $\nu' = 55.0$. Also, in this configuration the secondary vortices are no longer at fixed positions in the corners.

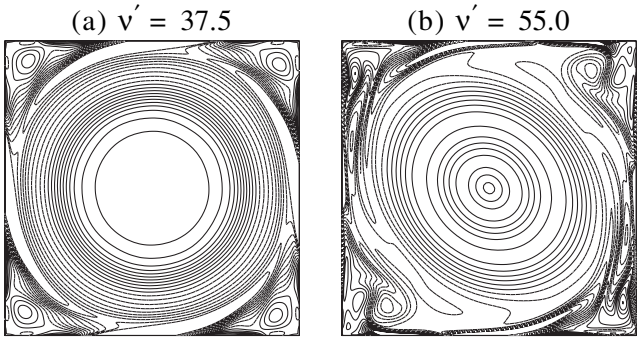

FIG. 1. Normalized isovorticity plots for time-periodic flows with rotational symmetry (a) over $\pi/2$ and (b) over π, for ν' as indicated. Contours range from -10 to 10 with an interval of 1, and dashed lines represent negative values.

The no-slip boundaries seem to stabilize the flow configuration, as on a square domain with periodic boundary conditions a similar symmetry breaking was already found to occur in the steady regime, when moving from the first to the second branch of steady solutions, whereas the first time-dependent solution in that case consists of traveling waves [10].

At the onset of periodic motion, peaks occur in the power spectrum of a point-measured vorticity time series at the basic frequency $f_1 \simeq 0.751$ and its integer multiples $2f_1$ and $3f_1$. For subsequent motions in the periodic state several higher harmonics are also excited, as shown for $\nu' = 40.0$ in Fig. 2(a). Evolution of the basic frequency f_1 as a function of the control parameter, given in Fig. 3, is seen to oscillate for the periodic state.

A secondary Hopf bifurcation leads to two-frequency quasiperiodic flow, observed in the interval $57.5 \leq \nu' \leq 65.0$. Here, spectral peaks occur at linear combinations of f_1 and the second basic frequency f_2, Fig. 2(b), where the winding number [19], $W = (f_2/f_1)$, is irrational. The value of the largest basic frequency increases monotonically as a function of the control parameter ($\nu' > 57.5$), as can be seen in Fig. 3, whereas the smallest basic frequency remains close to constant at $f_2 \simeq 0.26$.

At $\nu' = 67.5$ the system has entered a branch of flows for which the two basic frequencies are locked into a state with a rational winding number. For this frequency-locking interval $W = 1/3$, corresponding to a 1:3 Arnold tongue [19].

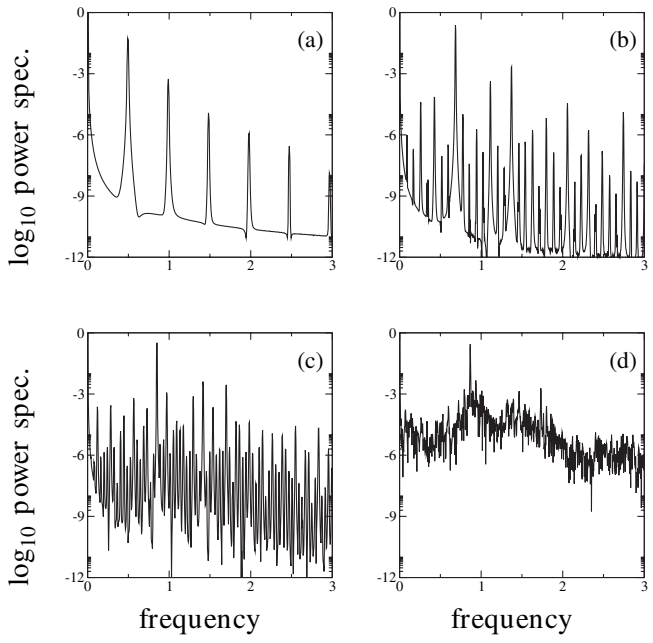

FIG. 2. Power spectra of vorticity time series for (a) periodic flow, $\nu' = 40.0$; (b) flow on a 2-torus, $\nu' = 57.5$; (c) flow on a 3-torus, $\nu' = 77.5$; and (d) chaotic flow, $\nu' = 80.0$.

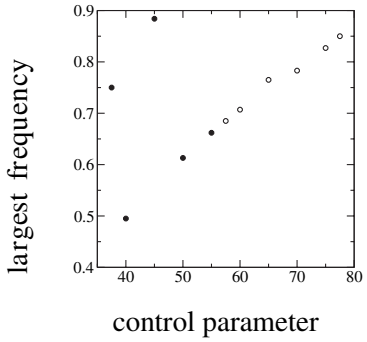

FIG. 3. Evolution of the largest basic frequency f_1 as a function of the control parameter ν'. Solid circles (●) symbolize period-1 flows, and circles (○) denote flows on a torus.

Quasiperiodic flow on the 3-torus is found for the parameter value $\nu' = 77.5$, shown in the form of a power spectrum in Fig. 2(c), where all peaks can be expressed as linear combinations of three basic frequencies, $f_1 \simeq 0.849$, $f_2 \simeq 0.445$, and $f_3 \simeq 0.285$.

Finally, within the interval $80.0 \leq \nu' \leq 85.0$ the temporal behavior of the flow is characterized by aperiodic fluctuations, resulting in a power spectrum with a broadband continuous component, Fig. 2(d). The presence of such a continuous component is a general indication of chaotic behavior [19].

Projections of the system attractor onto the $(\omega(t), \omega(t+\tau))$ plane are shown in Fig. 4, where the delay τ was determined from the average mutual information [20]. In each case phase space is reconstructed from a vorticity time series measured at location $\mathbf{x} = (1/2, 0)$. The dynamics can be sufficiently determined from such a single times series [21], and it was checked that time series measured at other locations in the domain yielded similar results.

The Poincaré return map plots the first coordinate of a point where the phase space orbit crosses a given (hyper)-plane against the first coordinate of the next crossing. For several values of the control parameter, Poincaré return maps are shown in Fig. 5.

At first, the two-frequency quasiperiodic flow fills a 2-torus, resulting in a closed-loop return map in Fig. 5(a). However, for $67.5 \leq \nu \leq 75.0$, the system enters a frequency-locking interval, for which the 2-torus is no longer filled by the dynamics. In the corresponding phase portrait, Fig. 4(a), it is seen that the orbit closes in on itself after three rotations in the long direction of the torus, whereas the winding number $W = 1/3$ indicates that the orbit simultaneously completes one rotation in the short direction. The flow lies on a period-3 cycle, for which the return map consists of three nodal points, Fig. 5(b).

Quasiperiodic flow on the 3-torus results in a complicated structure for the return map, Fig. 5(c), whereas for the chaotic state, no recognizable pattern can be distinguished, Fig. 5(d). However, a projection of the attractor, Fig. 4(c), has a structure comparable to a projection of the

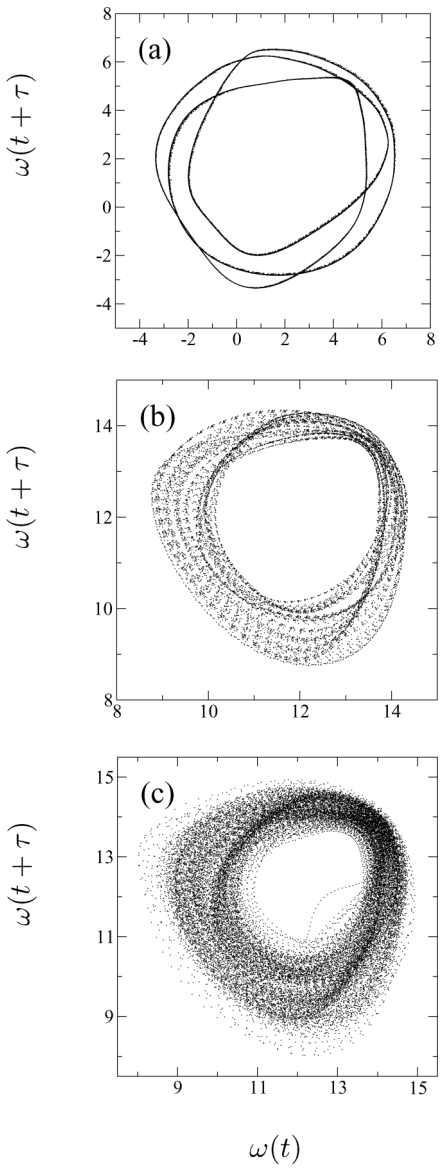

FIG. 4. Projection of the attractor onto the $(\omega(t), \omega(t+\tau))$ plane for (a) a period-3 flow, $\nu' = 70.0$; (b) flow on a 3-torus, $\nu' = 77.5$; and (c) a chaotic flow, $\nu' = 80.0$.

3-torus, Fig. 4(b), suggesting chaos arises due to the destruction of a 3-torus.

The correlation dimension, D_{corr}, is a measure of the (fractal) dimension of the attractor. Estimated according to Ref. [22], its value is approximately $D_{\text{corr}} \simeq 1.0$ for the single periodic flows. At the onset of two-frequency quasiperiodic flow the estimate equals $D_{\text{corr}} \simeq 2.2$, while the estimate drops to $D_{\text{corr}} \simeq 1.3$ for the branch of period-3 flows. For the three-frequency quasiperiodic flow $D_{\text{corr}} \simeq 2.9$, which is close to the expected value, whereas the chaotic motion results in slightly higher dimensions, at $D_{\text{corr}} \simeq 3.6$.

To summarize, a transition to chaos comparable to that described by the Ruelle-Takens-Newhouse scenario, is

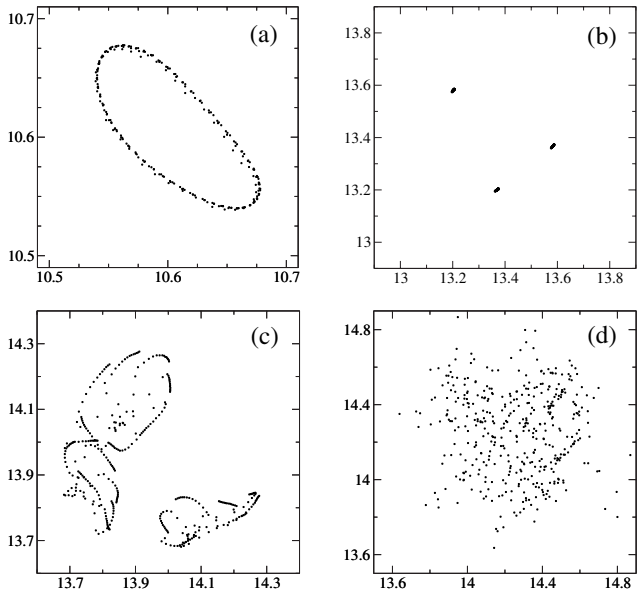

FIG. 5. Poincaré return maps, for (a) flow on a 2-torus, $\nu' = 57.5$; (b) a period-3 flow, $\nu' = 75.0$; (c) flow on a 3-torus, $\nu' = 77.5$; and (d) chaotic flow, $\nu' = 80.0$.

retrieved in a forced 2D flow on a square domain with no-slip boundaries, within the parameter range $25.0 \leq \nu' \leq 85.0$. Chaos arises through the destruction of a 3-torus. Moving from the ground state towards the chaotic solutions, spatial symmetry is reduced from the full symmetry group of the square to rotations about the center of the square over an angle π. For all these solutions the flow field is dominated by a large circulation cell, which appears during the secondary steady state, in a manner analogous to the appearance of rolls during the onset of steady convection. Overall, the transition sequence is not as rich as that found in a square domain with periodic boundary conditions [10]. Finally, the computations with no-slip walls form a crucial step in understanding results from laboratory experiments on quasi-2D flows.

One of us (D. M.) is grateful for support by the Foundation for Fundamental Research on Matter (FOM). The National Computing Facilities Foundation of The Netherlands (NCF) is thanked for the use of its supercomputers. J. Moehlis (University of California at Santa Barbara) is gratefully acknowledged for helpful comments.

[1] J. Sommeria, J. Fluid Mech. **170**, 139 (1986).
[2] J. Paret, M. C. Jullien, and P. Tabeling, Phys. Rev. Lett. **83**, 3418 (1999).
[3] S. R. Maassen, H. J. H. Clercx, and G. J. F. van Heijst, Phys. Fluids **14**, 2150 (2002).
[4] S. Li, D. Montgomery, and W. B. Jones, J. Plasma Phys. **56**, 615 (1996).
[5] H. J. H. Clercx, S. R. Maassen, and G. J. F. van Heijst, Phys. Rev. Lett. **80**, 5129 (1998).
[6] D. Molenaar, H. J. H. Clercx, and G. J. F. van Heijst, Physica (Amsterdam) **196D**, 329 (2004).
[7] G. K. Batchelor, Phys. Fluids Suppl. II **12**, 233 (1969).
[8] P. Tabeling, O. Cardoso, and B. Perrin, J. Fluid Mech. **213**, 511 (1990).
[9] R. Braun, F. Feudel, and P. Guzdar, Phys. Rev. E **58**, 1927 (1998).
[10] F. Feudel and N. Seehafer, Phys. Rev. E **52**, 3506 (1995).
[11] D. Ruelle and F. Takens, Commun. Math. Phys. **20**, 167 (1971).
[12] S. Newhouse, D. Ruelle, and F. Takens, Commun. Math. Phys. **64**, 35 (1978).
[13] G. Ahlers, Phys. Rev. Lett. **33**, 1185 (1974).
[14] J. P. Gollub and H. L. Swinney, Phys. Rev. Lett. **35**, 927 (1975).
[15] H. L. Swinney and J. P. Gollub, Phys. Today **31**, No. 8, 41 (1978).
[16] J. P. Gollub and S. V. Benson, J. Fluid Mech. **100**, 449 (1980).
[17] A. Libchaber, S. Fauve, and C. Laroche, Physica (Amsterdam) **7D**, 73 (1983).
[18] H. J. H. Clercx, J. Comput. Phys. **137**, 186 (1997).
[19] E. Ott, *Chaos in Dynamical Systems* (Cambridge University Press, Cambridge, U.K., 2002).
[20] H. D. I. Abarbanel, *Analysis of Observed Chaotic Data* (Springer-Verlag, Del Mar, 1996).
[21] J. C. Robinson, Proc. R. Soc. A **457**, 1007 (2001).
[22] M. T. Rosenstein, J. J. Collins, and C. J. D. Luca, Physica (Amsterdam) **65D**, 117 (1993).